

A practical approach to reactive ion etching

This content has been downloaded from IOPscience. Please scroll down to see the full text.

2014 J. Phys. D: Appl. Phys. 47 233501

(<http://iopscience.iop.org/0022-3727/47/23/233501>)

View the [table of contents for this issue](#), or go to the [journal homepage](#) for more

Download details:

IP Address: 129.94.115.114

This content was downloaded on 04/05/2015 at 08:39

Please note that [terms and conditions apply](#).

A practical approach to reactive ion etching

Fouad Karouta¹

Australian National Fabrication Facility, Research School of Physics and Engineering, Australian National University, Canberra, ACT 0200, Australia

E-mail: fouad.karouta@anu.edu.au

Received 14 December 2013, revised 27 March 2014

Accepted for publication 28 March 2014

Published 8 May 2014

Abstract

In this paper, general aspects of the reactive ion etching (RIE) technique will be described, such as anisotropy, loading effect, lag effect, RIE chemistries and micro-masking, followed by a brief overview of etching dielectrics (SiO_x , SiN_x) and crystalline Si. The second section of the paper is dedicated to etching III-V compound semiconductors where, based on RIE results of GaN material, a simple and practical thermodynamic approach is exposed, explaining the criteria for selecting the best chemistry for etching a specific material and explaining the GaN etching results. Finally, a comprehensive study of etching InP-based materials using various chemistries will be discussed, as well as their various photonic applications.

Keywords: RIE, loading and lag effects, micro-masking, GaN, GaAs, InP, nano-photonics

(Some figures may appear in colour only in the online journal)

1. Introduction

Plasma etching, dry etching and reactive ion etching (RIE) all describe processing techniques that have in common the fourth state of matter: plasma, also called the ionized state of material. The plasma state describes a condition where one or more gases are held at a certain pressure and submitted to an electrical potential, causing the partial ionization of the gas atoms [1]. In plasma, positive ions, radicals and electrons co-exist. About three decades ago, most industrial processes for semiconductor devices relied heavily on wet etching techniques; however, plasma processes, and more specifically RIE, gradually replaced wet etching techniques. This was due to their superior uniformity, repeatability and, more importantly, high throughput with the advent of equipment allowing batch processing.

The subject of dry etching has been extensively reported in the literature and covers various chemistries and materials spanning dielectrics (oxides and nitrides), polymers, semiconductor materials and even metals. There is a large variety of plasma reactors, each with its own particularity. The most common are as follows:

- Capacitively coupled plasma (CCP) reactor, where the feed gas is injected directly between two parallel plates (electrodes) while the chamber is maintained at a certain

pressure. If a radio frequency (RF) voltage is applied between the electrodes, the feed gas is ionized and the plasma obtained may be used for various etching processes. The lower electrode is characterized by a negative voltage concentrated in the so-called sheath layer where ions entering are accelerated proportionally to the lower electrode negative potential (often referred to as the direct current (dc) bias) and also to the ion charge. As a result the ions build up a kinetic energy that is lost when they hit the lower electrode (or sample to be etched). This ion energy is often essential in activating an etching process which is then called ion-driven etching. In such a system, pressure and gas flow directly affect the dc bias; however, RF power has the most influence on dc bias and an increase of RF power increases the dc bias and hence the ion energy. Although accelerated ions are indispensable for ion-driven etching they also introduce damage to the sample to be etched.

- Inductively coupled plasma (ICP) reactor, where the feed gas is ionized remotely and away from the lower electrode. The plasma in such a reactor is controlled by two high-frequency generators: one to ignite the plasma remotely with the second generator coupled to the lower electrode which induces the dc bias. Hence, in this reactor (also called the high-density reactor) it is possible to control the plasma density independently of the dc bias applied to the lower electrode. Traditionally, ICP discharges occur

¹ Previously with the Opto-Electronic Group, COBRA, Technical University Eindhoven 5600 MB Eindhoven, the Netherlands.

at lower pressures (compared to CCP discharges) and the power coupling occurs through a dielectric window or wall (made of quartz) and not directly to the lower electrode. This is the main factor resulting in a noticeably low voltage across all plasma sheaths at electrodes and walls.

For instance, increasing ICP power would lead to higher plasma density and simultaneously to lower dc bias. Therefore, ICP reactors are capable of achieving anisotropic etching at a much higher rate than CCP reactors. The process can be tuned to minimize the dc bias responsible for inducing damage to the etched sample surface. The dc bias in an ICP reactor can easily be tuned to be about 20–30% of the dc bias in a CCP reactor. As a result, it is widely accepted that average damage in ICP or similar high-density plasma reactors is much smaller than induced damage in CCP reactors.

Plasma can be characterized by various parameters:

- Plasma density typically 10^{15} – 10^{17} m^{-3} in CCP and one order of magnitude higher (10^{16} – 10^{18} m^{-3}) in ICP systems.
- Electron temperature of a few eV in both reactors.
- Ionization degree: 10^{-8} – 10^{-3} in CCP and 10^{-4} – 10^{-1} in ICP reactors (about four orders of magnitude higher).

Another type of high-density plasma reactor is the so-called electron cyclotron resonance (ECR). This type of reactor was very popular in the mid-80s and 90s but gradually lost ground to the newer ICP reactors that showed better reproducibility and equal (or superior) results for lower investment and running costs. ECR reactors required very powerful magnets to control and confine the plasma in the column prior to arriving at the lower electrode.

Particles present in plasma can collide, and this can be accompanied by various phenomena:

- change in energy;
- particle transformation (a neutral particle becoming ionized, or vice versa).

In a noble gas (e.g. argon) discharge, when an electron hits an ion the electron loses momentum (energy), whereas when an atom collides with an ion, energy is exchanged and a charge may be transferred. Similar processes occur in molecular gas discharge along with other important processes such as dissociation, positive–negative ion charge transfer and excitation of molecular vibrations. The frequency of these collisions depends mainly on the discharge pressure. To better understand this issue we need to define the so-called mean free path, defined as the average distance that a particle can travel without any collision:

$$\lambda = \frac{kT}{\sqrt{2\pi}d^2 p}$$

where k is Boltzmann's constant, d is the gas molecule diameter which varies slightly depending on the used gas, and T and p are the temperature and pressure of the medium.

At lower pressures, the mean free path becomes larger. For instance, at 1 mTorr, argon has a mean free path of about 5 cm. The benefit of lower pressures is the reduction in the chance

of collisions in the plasma leading to lower energy loss in the system and an improved contribution to the etching process.

This paper aims to give a practical approach to tackle matters related to plasma etching of various types of materials. Section 2 describes general aspects of RIE and important issues like anisotropy definition, loading effect, lag effect, dc bias reading, micro-masking and the appropriate choice of chemistry to etch a certain material. Section 3 gives a brief description of etching Si, SiO_x and SiN_x . Section 4 concentrates on etching III–V compound semiconductors in general and gives a detailed review of how the chosen chemistry can have a large impact on etching results using various physical and thermodynamic data. Finally, the RIE of InP-based materials is described for various photonic applications. All experimental data shown in the paper are carried out by the author.

2. General aspects of RIE

2.1. Anisotropy in dry etching

One aspect worthy of explanation is the interpretation of anisotropy in dry etching. In wet etching, anisotropic/isotropic etching indicates the etching process results in different shapes along different crystal orientations. Hence, isotropy means the same shape is obtained along all crystal orientations. The obvious example here is etching GaAs (001) in $\text{H}_3\text{PO}_4 : \text{H}_2\text{O}_2 : \text{H}_2\text{O}$ mixture, resulting in a V-grooved shape along the [0 1 1] direction and a dove-tailed shape along the [0 1 1] direction. Note that the V-planes (along [0 1 1]) and the dove-tail planes (along [0 1 1]) are identical. Both are (1 1 1)A facets distinguished as being terminated with a Ga atom or other III-elements atom which is bonded to three As (or other V-elements atom) located in the underlying layer. This leaves the Ga atom with no available electrons to establish any bonds and results in a higher chemical inertness of A facets in III–V semiconductors. As wet etching is the slowest at the (1 1 1)A facet and the fastest at (1 1 1)B which is As-terminated. However, in dry etching anisotropy/isotropy is not related to crystal orientation but to the resulting shape: 100% anisotropy means vertical etched sidewalls whereas 100% isotropy means spherical sidewalls as a result of equal vertical and horizontal etching, as demonstrated in figure 1. As discussed later, anisotropic etching is obtained when sufficient sidewall passivation takes place during the etching process.

2.2. Loading effect

This effect associated with RIE processes describes how the etching depth and rate may vary with the total surface area exposed to etching [2, 3]. This can be elucidated by the faster depletion of reactants with larger surface areas to be etched as compared to when only a small piece of the same material is exposed to an RIE process. However, this effect is very dependent on the chemistry used (i.e. the gases), the chamber configuration and, more importantly, the material forming the lower electrode. When the material of the lower electrode can be etched with the chemistry used, the loading effect on the real samples to be etched is minimized. This is due to the

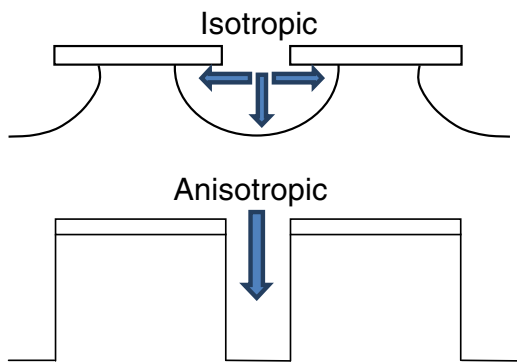


Figure 1. Schematic of isotropic versus anisotropic plasma etching.

simple fact that the reactants will react with both the samples to be etched and with the electrode material. This larger, combined, exposed surface contributes to the elimination of the loading effect. This is demonstrated with practically identical etching rates when etching Si using either a graphite or a Si electrode, and the etching rate of Si sample edges doubling when using a Styron electrode [3]. The loading effect should be considered when etching InP-based materials in $\text{CH}_4 : \text{H}_2$ plasma discharges with a lower electrode made of quartz. Quartz is practically insensitive to $\text{CH}_4 : \text{H}_2$ discharges, resulting in the reactants migrating along the electrode surface until they make contact with the InP material. In these conditions, etching a $1 \times 1 \text{ cm}^2$ InP sample would result in a much higher etching depth compared to the situation where a full 2 inch InP wafer is etched. Also, and as reported in [3], the etching rate at the edges of the sample would be higher than in the middle. In such cases, the way to circumvent this problem is to use, at all times, a sacrificial sample of the same material (e.g. a 2 inch InP wafer), onto which the effective small piece can be positioned. In this way the etching rate is determined by the total surface area which is now formed by the 2 inch wafer. Even using different sample sizes results in the total surface area exposed to the plasma process remaining practically constant, resulting in fairly constant and reproducible etching rates. A similar effect can occur when etching samples of equal size but differing in the size of the exposed area: a $2 \times 2 \text{ cm}^2$ sample with a 10% opened area (through a mask) will etch much faster than the same size sample ($2 \times 2 \text{ cm}^2$) presenting an opened area of 90%. As stated earlier, the loading effect strongly depends on the chemistry, chamber configuration and the lower electrode material. Experiments reported in [2, 3] deal with a parallel plate reactor. In most ICP reactors, a Si carrier wafer is used, onto which small size samples are positioned or fixed. Depending on the chemistry used, the loading effect tends to be much reduced, especially when the Si carrier wafer is etched at the same time. This is particularly true in fluorine-based chemistry where etching rates of SiN_x or SiO_x samples are independent of sample size if placed on a Si carrier wafer, as the carrier wafer is also etched in this chemistry. The loading effect is also reduced in an ICP reactor using Cl_2 -based chemistry, as the Si carrier wafer is also etched by chlorine radicals.

2.3. Lag effect

The RIE lag effect is a qualification given to the difference in etching depth resulting from the feature size. When etching through varying opening sizes in a mask, for example, the etch depth can be much larger in large, open areas compared to smaller size openings. This non-uniform etching is related to the diffusion processes of etching reactants and products to and from the etched hole: the smaller the size, the longer the time required for the reactants to reach the bottom of the hole. Similarly, longer times are required for the outward diffusion of the etching products. Figure 2 illustrates this RIE lag effect very well, showing an SEM photograph of an ICP-RIE etching process using $\text{Cl}_2 : \text{Ar} : \text{H}_2$ to etch InP. The patterns consist of straight lines (trenches) with varied width from $1 \mu\text{m}$ down to 100 nm in 100 nm steps with the gaps between trenches varying accordingly. It is worth noting that the decrease in etching depth at the smallest openings (300 nm and below) is dramatic.

2.4. Dc bias in CCP and ICP systems

In a capacitively coupled (CCP) reactor when a certain discharge is created, the RF power applied to the lower electrode is directly related to the so-called dc bias: a negative potential responsible for attracting positive ions to the electrode at an impinging energy proportional to the ion charge and the electrode potential. When increasing the RF power the plasma becomes denser and an increase in the dc bias also occurs. Hence, in such reactors the plasma density is associated with a higher dc bias, thus producing a higher ion bombardment. This situation is very different in an ICP reactor where two RF generators are used: one at 13.56 MHz connected to the ICP source and a second that may also operate at 13.56 MHz connected to the lower electrode. In this situation the plasma density is dissociated from the dc bias, as increasing the ICP power would result in a higher plasma density, but a moderate RF power will result in a fairly low dc bias. It is well known that high-density plasma reactors, like an ICP system, induce far less damage to the etched surface. Additionally they have the potential to offer anisotropic etching (close to vertical sidewalls) whereas regular RIE systems often result in slanted sidewalls.

2.5. Micro-masking

Micro-masking is usually a non-desired phenomenon that may accompany plasma etching processes under certain conditions. The most frequently encountered micro-masking occurs when a metal mask is used. During such etching, the physical sputtering of small metal particles, which are not volatile, may be re-deposited elsewhere on the sample and create micro-masking. Such a masking would result in randomly positioned etched structures of various shapes but mostly like dispersed nano-pillars. In recent years and due to the attention nanowires are gaining, researchers have been looking at alternatives using the top-down approach that usually require electron-beam lithography (EBL) techniques to define the position, and shape, of the nano-pillars to be etched. Alternatively there is

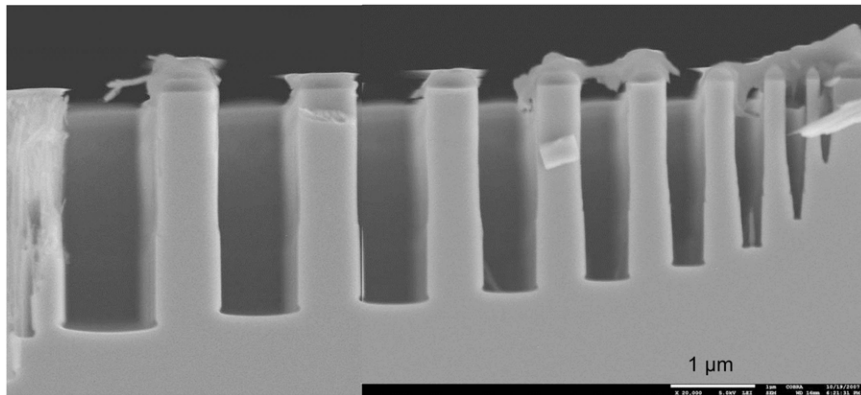


Figure 2. RIE lag illustrated when etching an array of trenches with varied widths from $1\text{ }\mu\text{m}$ down to 100 nm in 100 nm steps. Down to 300 nm trenches the etching rate decreases monotonically whereas below 300 nm the decrease of etching depth becomes exponential.

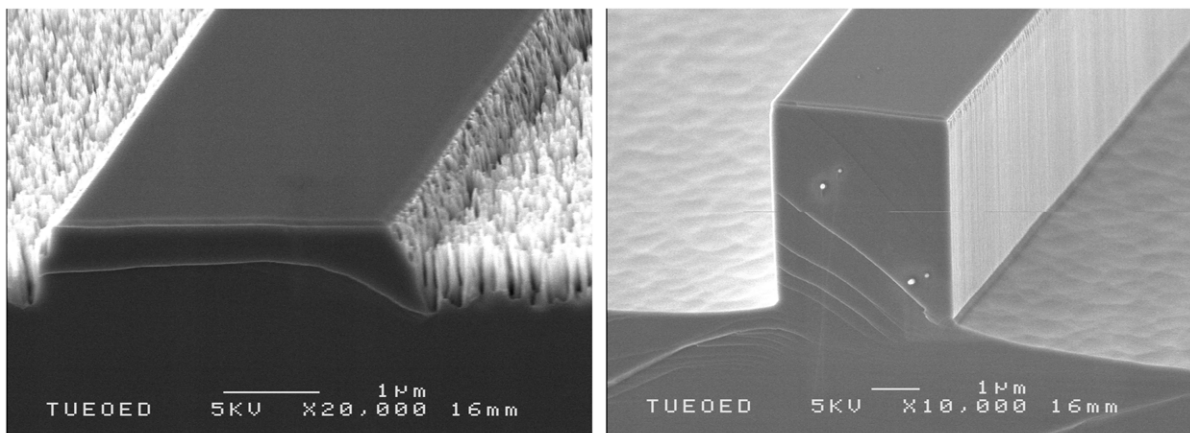


Figure 3. Micro-masking caused by the low volatility of the etching product InCl_3 when etching InP in $\text{Cl}_2\text{-Ar-H}_2$ (7, 4, 12 sccm), $T = 60^\circ\text{C}$, ICP = 1000 W, RF = 120 W for 2 min with HSP (left) and without HSP (right). Reproduced with permission from [37]. Copyright 2005 IEEE.

a report that makes use of a type of micro-masking to create the etched nano-pillars without the use of the expensive EBL technique [7].

Before proceeding further with micro-masking, a special note should be made as to the system layout: most modern ICP reactors make use of the so-called back-side He cooling. With this layout the reactor is constructed such that a quartz clamp pushes the carrier wafer towards the lower electrode and He pressure is maintained between the two surfaces to ensure good thermal conductivity. This ensures that the energy given by the plasma is not heating the lower electrode during etching and, hence, the sample to be etched. When etching small pieces (which is often the case with III-V materials in research institutes) the small sample is positioned on the carrier wafer using a heat conductive adhesive (heat sink paste, or HSP) or fomblin oil. Here again, the paste/oil ensures that the sample is at a temperature very close to that of the lower electrode, and in this case the sample is thermally coupled to the lower electrode. If the sample is placed on carrier wafer without any paste/oil then the sample is no longer thermally coupled; this situation also arises if no He is used between the carrier wafer and the electrode. In these cases, and depending on the RF and ICP power, the sample can be heated to temperatures beyond 200°C in just a few seconds while the electrode

temperature is only 60°C . It has been reported that the effect of heating the electrode by increasing the ICP power from 400 to 800 W resulted in an increase of substrate temperature from 70 to 110°C [4]. In this paper two types of micro-masking phenomena will be described:

- *Micro-masking caused by the slow volatility of an etching product.* A typical example of this phenomenon is when etching InP in the Cl_2 -based chemistry and the creation of the etching product InCl_3 , which is not highly volatile. From the *Handbook of Physics and Chemistry* [5] we can find that the boiling point (T_B) of InCl_3 is about 600°C at 1 atm. This medium T_B value is an indication that additional care is required when etching In-containing materials. As the vapour pressure of InCl_3 is about 4 mTorr at 160°C it means that one possibility to avoid the micro-masking is to heat up the lower electrode on which the sample is placed. Typically, the etching of InP materials is carried out at an electrode temperature between 150 and 180°C . Figure 3 shows the obvious proof of the electrode temperature effect on the etching process: the left image shows a very rough InP surface presenting a multitude of whisker-like pillars after etching at 60°C (lower electrode) in $\text{Cl}_2 : \text{Ar} : \text{H}_2$ ambient (RF/ICP power

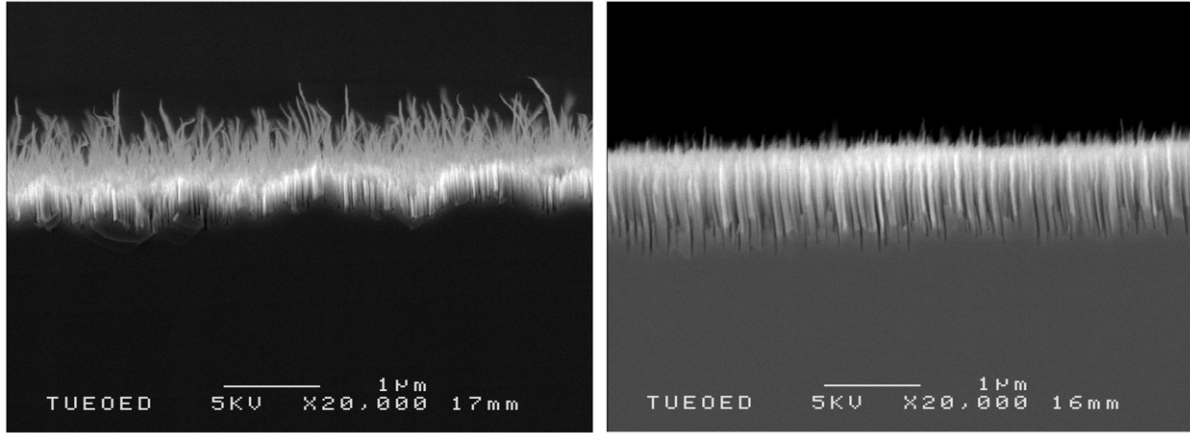


Figure 4. Micro-masking resulting from ICP etching using $\text{Cl}_2 : \text{CH}_4 : \text{H}_2$ at ICP/RF 1000/100 W for 3 min (left) and 4 min (right). Reproduced with permission from [7], Copyright 2005 IEEE.

of 100/1000 W) with He back-side cooling and HSP, while the image on the right shows a very smooth etched InP sample etched at the same time; the sole difference being that the heat conductive paste was not used.

Moreover, tests carried out with heat indicator tapes have shown that under the same process conditions the sample temperature rises to more than 200°C in less than 20 s [6] using $\text{Cl}_2 : \text{O}_2$ chemistry at an RF/ICP power of 160/1000 W. In conclusion, when using an ICP reactor without heating the electrode, smooth etching of InP is still possible with samples not thermally coupled to the electrode (i.e. with no He flow and no conductive paste). With a $\text{Cl}_2 : \text{CH}_4 : \text{H}_2$ chemistry the micro-masking effect was absent when etching InP at 60°C electrode temperature with or without heat conductive paste. It is likely that In is evacuated either as trimethyl indium or an intermediate form between trimethyl indium (TMIn) and InCl_3 , which is volatile at 60°C and 4 mTorr pressure.

- *Substrate and chemistry-initiated micro-masking.* This micro-masking occurs under fundamentally different conditions and is not related to the low volatility of an etching product. This phenomenon started when trying to etch semi-insulating (s.i.) InP placed on a 4 inch Si wafer (hence without HSP) in a load-locked Oxford Plasma Lab 100 ICP system using $\text{Cl}_2 : \text{CH}_4 : \text{H}_2$ chemistry (7:8:5.5 sccm) at an electrode temperature of 60°C (RF/ICP 100/1000 W at 4 mTorr). After 3 or 4 min of etching, the sample was completely black due to a full coverage of whiskers, as shown in figure 4. SEM analysis showed two whisker shapes for the sample etched for 3 min: solid whiskers in the bottom part (1/3 height) and hairy whiskers in the top part, whereas in the sample etched for 4 min solid whiskers are dominant with only short tails of hairy whiskers visible. The whisker size was typically about 100 nm in diameter and 2–3 μm long [7]. This micro-masking effect was completely absent when etching, under the same conditions, conductive InP substrate (n- or p-type material). Figure 5 shows SEM micrographs of the n-InP, p-InP and the s.i. InP samples etched at the same time under the same process conditions

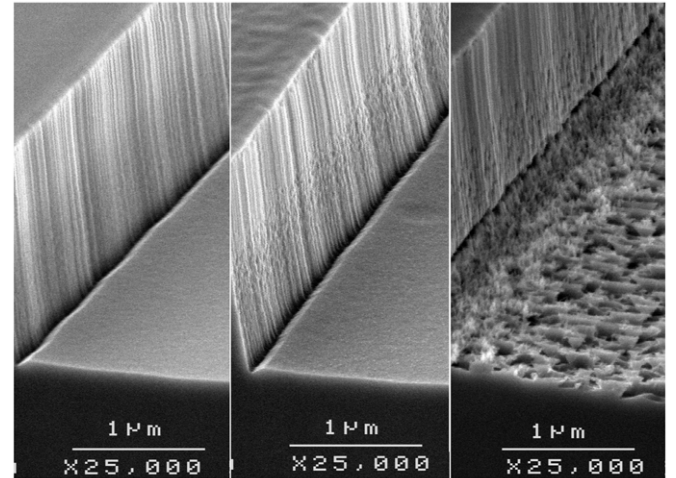


Figure 5. Comparison of etching results on n-InP (left), p-InP (middle) and s.i. InP (right) under the same process conditions. Reproduced with permission from [7], Copyright 2005 IEEE.

for 90 s. The n-type InP shows a clean and smooth etched surface while the s.i. InP shows a very rough etched surface. The fact that micro-masking was only occurring with s.i. InP suggests that electric fields within the plasma sheath are strongly affected by the electrically isolated s.i. InP material, which led to the build-up of surface roughness resulting in this auto-initiated micro-masking. It is worth noticing that the process does etch n-InP at $1.2 \mu\text{m min}^{-1}$.

Several additional experiments were performed to identify the reason for the micro-masking or at least to identify a way to avoid it. We first ran a series of a few samples proceeding in multiple cycles with an identical total etching time of 3 min but varying the cycle time from 30 to 45 to 60 s. All of these samples were free of any micro-masking; however, they all presented a rough surface. Knowing that etching in multi-cycles would reduce the temperature heating of the sample during the etching process, it is assumed that the major cause of the micro-masking is the heating effect. A second test sample was

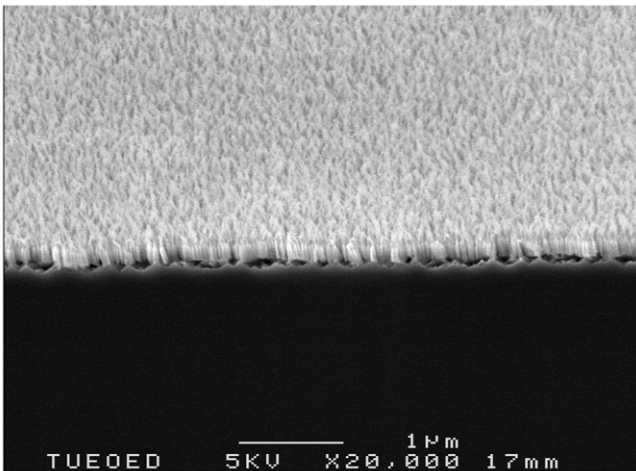


Figure 6. Very short solid whiskers were obtained when etching a sample protected with a 400 nm SiN_x layer ensuring sufficient sample heating during removal of the nitride masking layer.

etched for 4 min under the same conditions using a s.i. InP sample covered with a 400 nm SiN_x masking layer. From previous work we knew that a 400 nm nitride layer would survive the etching process for about 3 min and 20 s, hence the InP would only be etched for approximately 40 s after etching away the SiN_x layer. During this time the sample was heated sufficiently to create the micro-masking effect, resulting in etching showing solid whiskers much shorter than before, as shown in figure 6.

This agrees with the former findings that the micro-masking accompanies the heating up of the sample under the plasma effect.

A final experiment was carried out using two s.i. InP samples; one with HSP and second sample simply placed on the Si wafer. After 4 min etching under the same conditions, the sample with HSP revealed a shiny and very smooth surface while the as-placed sample turned black, as can be seen in figure 7.

Knowing that the difference between the two samples is due to the temperature evolvement, we can conclude that the whiskers were formed due to the excessive heating of the as-placed sample, whereas the thermally coupled sample with a temperature very close to that of the electrode (60°C) was devoid of whiskers. This excessive heating likely resulted in the polymerization of the CH_4 into larger molecules, causing the micro-masking and generating the whiskers. However, it is not clear why only the s.i. InP is subjected to this excessive heating whereas conductive InP substrates have shown a smooth etched surface. It is worth noting that etching s.i. InP for the much longer time of up to 7 min did not result in longer whiskers.

This indicates the micro-masking is self-limiting and the whiskers move downward into the substrate, but once the whiskers are formed they evidently remain present. Finally, also worthy of note is the fact that the blackened s.i. InP with whiskers has shown much higher photoluminescence signal intensity, a few orders of magnitude greater than non-etched s.i. InP [7].

2.6. Choice of chemistry

Three basic chemistries are dominating dry etching techniques: chlorine-based, fluorine-based and the methane–hydrogen combination. Numerous variations are derived from these chemistries depending on the material to be etched and the objective/application. Described below is a simple approach that helps in determining the correct chemistry for dry etching of any substance:

- (1) A successful dry etching chemistry should produce volatile etching products. This is best described by the vapour pressure of the product associated with a certain temperature. For instance, the etching product of InP using Cl_2 -based chemistry is InCl_3 , which has a vapour pressure of 4 mTorr at 160°C . This means that InCl_3 will not become volatile until the pressure is 4 mTorr or lower and the temperature is 160°C or higher. A more practical way would be to look at melting/boiling points of possible etching products associated with the substance to be etched. If the melting point (T_m) and/or boiling point (T_b) are in the order of a few hundred degrees it is then likely that the substance can be etched with the associated chemistry. This is strongly dependent on the temperature and pressure of the etching process (see section 3).
- (2) Determine the most adequate masking material: SiO_x or SiN_x layers, photo-resists, metals or other, e.g. a combination of 2–3 of the masking materials mentioned above.
- (3) Once the chemistry is determined, the electrode temperature and pressure need to be determined to allow a swifter (smoother) etching process. If the volatility of the expected etching products is medium to high, the etching can be enhanced if the sample and electrode are set at a higher temperature associated with a lower pressure.
- (4) Finally, the optimum plasma power needs to be investigated and determined. In an ICP reactor there are two variables—RF and ICP power—which both influence the dc bias reading. When ICP is increased the dc bias decreases, whereas the dc bias increases with increasing RF power at constant ICP power.

Although Si is often dry etched using fluorine chemistry, chlorine can be added to the chemistry to enhance the etching anisotropy [8]. III–V compound semiconductors show different behaviours to Si. For instance, GaAs and InP can both be etched using the CH_4 – H_2 combination as this chemistry offers well-controlled and low etching rates. Generally, fluorine chemistry is not suited to etching III–V materials as the fluorides of elements III are not volatile. Hence, etching a SiO_x mask with the F-based chemistry is highly selective towards InP and GaAs. One particular application is photonic bandgap structures, also called photonic crystals (PhC), which are periodic structures created in semiconductor materials. PhC structures require etched holes that are smooth and have high aspect ratios. To achieve this, chemistries based on Cl_2 are required in association with other gases like H_2 and O_2 or Ar.

Cl_2 -based chemistry is practically a universal etchant for many substances, with the exception of a few metals, and is

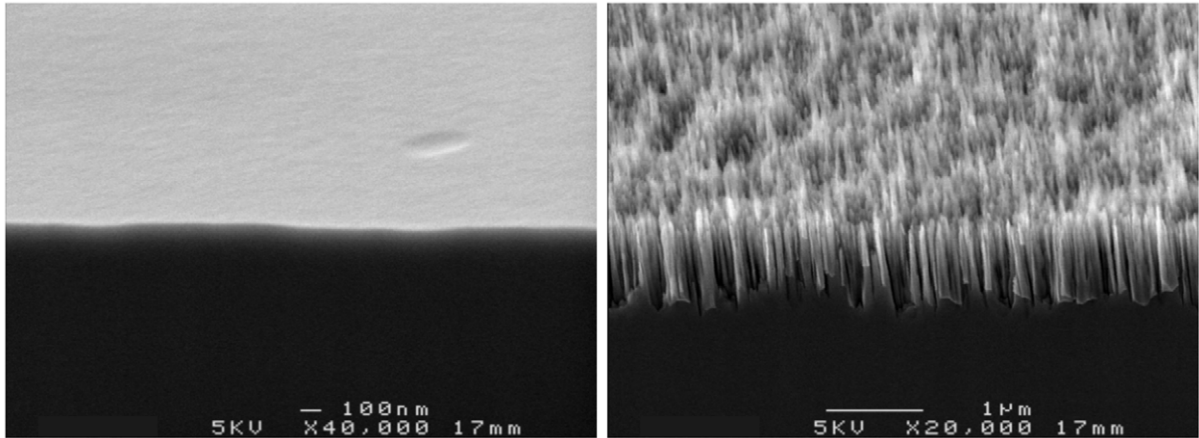


Figure 7. SEM photographs of two InP samples etched simultaneously. The left sample shows a very smooth etched surface due to the use of HSP on the Si wafer compared to the right sample simply placed on the Si wafer—whisker growth is due to excessive heating from the plasma. Reproduced with permission from [37], Copyright 2005 IEEE.

widely used in dry etching of III–V compound semiconductors. However, it is rare to use Cl_2 alone and combinations with other gases are generally used, depending on the etched material system and applications. The most common combinations are $\text{Cl}_2 : \text{CH}_4 : \text{H}_2$ and $\text{Cl}_2 : \text{Ar} : \text{H}_2$. When one of the III elements is indium, the electrode temperature becomes an important factor in the etching process as InCl_3 is not very volatile, and to enhance its volatility it is common practice to increase the electrode temperature along with lowering the pressure. This is required with both $\text{Cl}_2 : \text{CH}_4 : \text{H}_2$ and $\text{Cl}_2 : \text{Ar} : \text{H}_2$ chemistries.

When comparing specific chemistries for etching two different materials it is logical to expect that the etching rate of the material with the highest bond energy would etch at the lowest rate. For instance, $\text{Cl}_2 : \text{H}_2 : \text{Ar}$ can be used to etch many III–V semiconductors; however, under the same plasma conditions the etching rate of GaN would be lower than the etching rate of GaAs simply because more power is consumed to break the strong Ga–N bond compared to the weaker Ga–As bond.

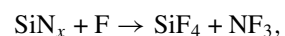
3. Dry etching of Si, SiO_x and SiN_x

Although dry etching of Si (and its dielectric derivatives) is of large importance in the Si microelectronics industry, this section has been deliberately kept limited. There are numerous papers reporting on plasma etching of Si, SiO_x and SiN_x [2, 3, 8]. The CHF_3 flow plays a crucial role in the quality of the etching surface as a too small CHF_3 flow will result in very rough Si surface (also called black silicon), as demonstrated by Legtenberg *et al* [3]. Based on tuning the isotropy of the etching process, and due to the bio-compatibility of Si, researchers have demonstrated the fabrication of micro-needles, $150\ \mu\text{m}$ long and with a $1\ \mu\text{m}$ tip, using a well-balanced (anisotropic versus isotropic) etching process based on $\text{SF}_6 : \text{O}_2$ [9].

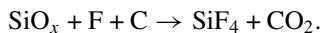
Si, poly and amorphous Si, SiO_x and SiN_x are commonly etched in a fluorine-based chemistry where the etching product is mainly volatile SiF_4 . Hence, a decent etching rate can be achieved in these materials depending on the reactor, the

exact used chemistry and the applications. Depending on the exact circumstances, different variations can be thought of, such as CHF_3 and SF_6 for etching Si, where SF_6 is the main chemical agent and CHF_3 provides some passivation, enabling an anisotropic etching. In this category, the Bosch process is the most known. It requires a mixture of two gases where one ensures a good etching of the material while the second creates a passivation layer to inhibit sidewall etching. SF_6 is the gas chosen for the fast etching of Si while C_4F_8 is the passivation gas. In the Bosch process [10, 11], the two gases are alternated and typically SF_6 is run for 7–8 s at lower pressure (to produce vertical etch) while C_4F_8 is run for 2–3 s at higher pressure to enhance the sidewall passivation. Hence, the latter creates a thin protective layer on the wafer horizontal surface as well as on the etched sidewall. When SF_6 is introduced, a very short time is dedicated to removing the bottom passivation layer followed by Si etching during the remaining time, which is the time required to etch away the passivation layer on the sidewall. Thus, repeating this cycle the necessary number of times ensures deep vertical etching as used in via holes. A very common chemistry to etch Si is based on $\text{SF}_6 : \text{O}_2 : \text{CHF}_3$, where anisotropic etching is achieved by tuning the flows of the three gases in parallel to the pressure and RF power [3]. In this process it was also found that, at reduced CHF_3 flow, the etched surface was very rough while a medium to higher CHF_3 flow contributed to a smoother etched surface. However, anisotropy was achieved where O_2 and CHF_3 were contributing to the passivation processes at the correct pressure (100 mT) and RF power (100 W).

As for etching SiO_x and SiN_x the most commonly used chemistry is based on CHF_3 plasma with an incidental addition of a small amount of oxygen to avoid a too strong polymer deposition. However, when using an EBL resist like PMMA or ZEP, the resistance to a mixture of $\text{CHF}_3 : \text{O}_2$ plasma is weakened significantly and the EBL resist is etched away quickly. Hence, in these circumstances CHF_3 can be used alone. The etching reactions can be written as



where both etching products are volatile.



Other gas alternatives for etching SiO_x and SiN_x are CF_4 and C_4F_8 , whereas SF_6 is rather used to etch nitride layers for the simple reason that C-radicals are then required to react with the O-atoms of the oxide layer to form the volatile CO_2 . Hence, SF_6 appears to be a good option for a selective etching of SiN_x over SiO_x . A few experiments were carried out in a load-locked Versaline Plasma Therm system to etch PECVD SiN_x and SiO_x layers deposited at 300 °C. When using pure SF_6 (40 sccm) or a mixture of $\text{SF}_6 : \text{O}_2$ (40 : 10 sccm) the etching rate of SiN_x was 2.4–2.5 times the etching rate of SiO_x (100/400 W RF/ICP power). During this process the measured dc bias was 224 V; however, a slightly higher selectivity of 2.70 : 1 was achieved when using higher ICP power (1000 W) and a lower RF power (30 W), resulting in a decreased dc bias of 44 V.

4. Dry etching of III–V semiconductors

In contrast with Si, III–V semiconductors cannot be etched at all with fluorine-based chemistry for the simple reason that fluorides of all elements III have extremely low volatility and as such no etching can take place. It is however worthy to note that fluorides of all elements V are very volatile. This property is attractive to exploit when etching III–Vs using a gas mixture of chlorine and fluorine shown in the sections below.

4.1. Dry etching of GaN

GaN is a wide bandgap material and has become the material of choice among III–V semiconductors. This is due to the industrial potential of this material system in optoelectronics (LEDs, solid state lighting, Blu-ray) and in microelectronics (high-power, high-frequency transistors). However, GaN has a high bond energy making it impossible to wet etch this material system. Hence, the only viable option to pattern this material is plasma etching, using a chlorine-containing gas to ensure a decent and repeatable etch. There are numerous papers on the subject of etching GaN and related materials but only a few of them report the use of combined chlorine–fluorine chemistry. The etching products of GaN in a Cl_2 -based chemistry are GaCl_3 and NCl_3 . Both of these products are volatile and hence etching GaN in Cl_2 , SiCl_4 or BCl_3 is straightforward. The results reported below all come from experiments conducted in a load-locked plasma lab 100 (capacitive coupling) from Oxford Plasma Technology. Our first etching experiments made use of $\text{SiCl}_4 : \text{Ar}$ (10 : 10 sccm) at 40 mTorr and at an RF power of 105 W ($\sim 0.32 \text{ W cm}^{-2}$). Smooth surfaces and an etching rate of 22 nm min^{-1} were observed. Then we investigated adding SF_6 (present in the system) to the $\text{SiCl}_4 : \text{Ar}$ mixture. Astonishingly, even when adding a small amount (2 or 4 sccm) of SF_6 , it resulted in a four-fold increase of the GaN etching rate, as shown in figure 8. At the same time the resulting etch shows very smooth surfaces, much smoother than the original epitaxial GaN layers grown on a sapphire substrate, as demonstrated in figure 9.

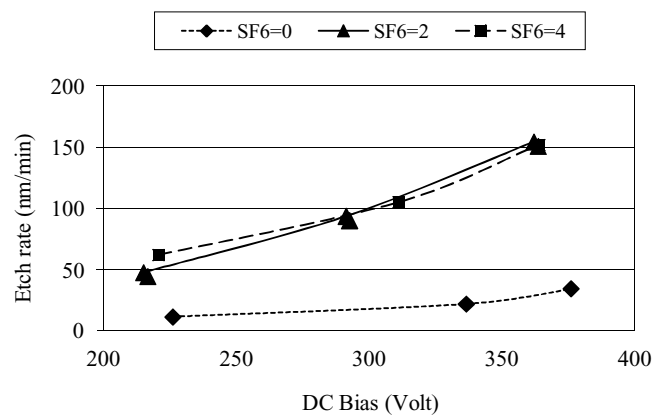


Figure 8. Etch rate of GaN as a function of SF_6 flow. Reproduced with permission from [14], Copyright 1999 The Electrical Chemical Society.

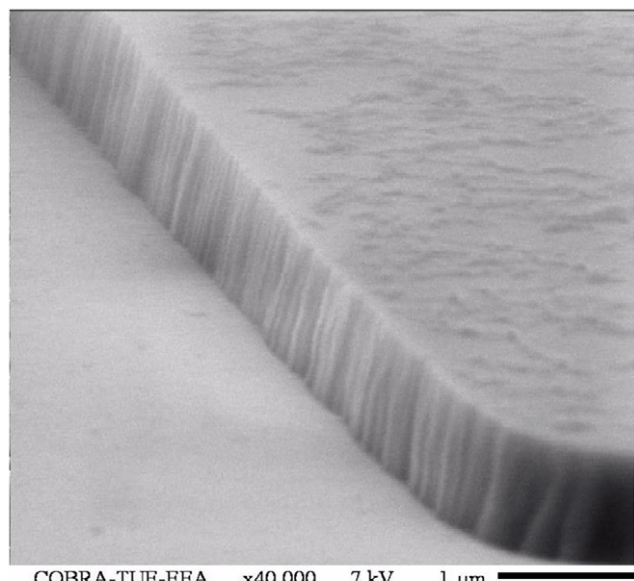


Figure 9. Very smooth surface after etching with $\text{SiCl}_4 : \text{Ar} : \text{SF}_6$. Reproduced with permission from [14], Copyright 1999 The Electrical Chemical Society.

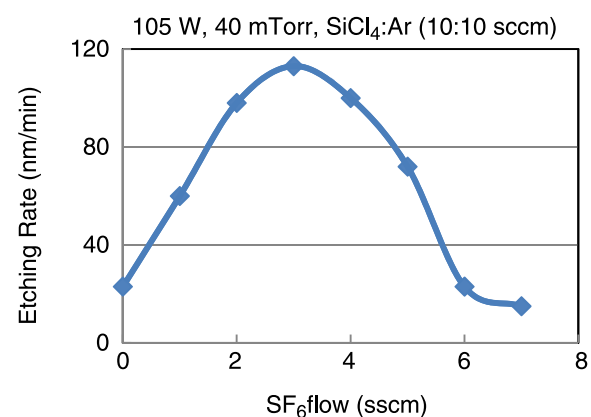


Figure 10. Etch rate of GaN as a function of SF_6 flow. Note at 7 sccm SF_6 flow the etching rate is even lower than the etching rate without any SF_6 . Reproduced with permission from [15], Copyright 1999 Wiley.

Table 1. Comparison of experimental data for etching GaN in chlorine and fluorine mixture.

RF power (W)	RF density (W cm^{-2})	Chemistry	Rate (nm min^{-1})	Added fluorine	Rate (nm min^{-1})	Reference
300	0.72	$\text{SiCl}_4 : \text{Ar}$	50	SiF_4	50	[12]
300	0.48	$\text{BCl}_3 : \text{Ar}$	50	SF_6	210	[13]
300	0.92	$\text{SiCl}_4 : \text{Ar}$	95	SF_6	>400	[14, 15]

When looking more thoroughly into the addition of SF_6 to SiCl_4 we found the etching rate versus SF_6 flow showed a Gaussian-like shape, as shown in figure 10. Moreover, two papers found in the literature reported the addition of a fluorinated gas to the chlorinated gas for etching GaN. Adesida *et al* [12] reported a 50 nm etching rate of GaN at 300 W RF power using $\text{SiCl}_4 : \text{Ar}$, and the etching rate remained unchanged when SiF_4 was added to the mixture. Feng reported a four-fold increase of the etching rate when adding SF_6 to $\text{BCl}_3 + \text{Ar}$ [13]. These two papers are very important and helpful in our attempt to understand the obtained results. The four-fold increase in the etching rate was particularly interesting as it is identical to the increase we experienced when adding SF_6 to the $\text{SiCl}_4 : \text{Ar}$ mixture. The results of the three works are summarized in table 1 and include the maximum etching rate reached at the maximum RF power of 300 W. However, for the sake of better comparison we also noted the RF power density (total power/electrode surface area), as the RF power in itself is not a relevant parameter in this comparison due to the influence of the reactor geometry and the lower electrode dimensions:

Three phenomena need clarification:

- (1) The four-fold increase of etching when adding a fluorinated gas to chlorine-based chemistry.
- (2) The collapse of the GaN etching rate at higher SF_6 flow.
- (3) The unchanged GaN etching rate when adding SiF_4 [12].

To explain the four-fold increase of etching rate when adding SF_6 , the first logical possibility may be attributed to a higher volatility of the etching products. For this, let us consider the boiling temperatures of all possible etching products—those are as follows:

- GaF_3 with a boiling point of about 1000 °C,
- GaCl_3 with a T_B of 201 °C,
- NF_3 (T_B of -129 °C) and
- NCl_3 with a T_B of 70 °C.

Obviously GaF_3 is a non-volatile product and needs to be avoided. GaCl_3 is quite volatile and it is also clear that NF_3 is much more volatile than NCl_3 . So, when etching GaN in a Cl_2 -based gas, the etching products are GaCl_3 and NCl_3 . In our case, where a small amount of SF_6 is added to the chlorinated gas, a four-fold increase of etching rate was reported [13, 14]. This important increase can only be explained by a different regime reached whenever the added SF_6 is quite limited (2–4 sccm SF_6 for 10 sccm SiCl_4 [15]). In this particular regime the etching products become GaCl_3 (for Ga) and NF_3 (for N). Another physical property that we need to consider is the enthalpy formation of the etching products. In addition to the fact that NF_3 is much more volatile than NCl_3 , the

enthalpy formation of NF_3 ($-31.4 \text{ kJ mol}^{-1}$) is also lower than that of NCl_3 (232 kJ mol^{-1} [16]), which explains why NF_3 is preferably formed instead of NCl_3 .

This particular behaviour is not restricted to GaN. The effect of combining Cl- and F-based chemistries seems to also produce a similar enhancement of the etching rate in GaAs [17] as well in Si [8]. Similarly to GaN, the etching rate increase of GaAs or Si can be attributed to the lower T_B of AsF_3 (60.4 °C) with respect to the T_B of AsCl_3 (130 °C) or to the higher volatility of SiF_4 ($T_B = -86^\circ\text{C}$) versus SiCl_4 (T_B of 57 °C).

However, there is a major difference between the case of III–V semiconductors and that of Si. In III–V, at higher fluorine flow another regime is then reached where it is likely that GaF_3 is formed instead of the more volatile GaCl_3 , slowing or even prohibiting the etching of the semiconductor material such as GaN [14] or GaAs [17]. When etching Si, adding or substituting more fluorine in the combined chemistry leads to a steady and continuous increase in the etching rate associated with loss of anisotropy [8].

The fluorine–chlorine combination is beneficial for etching GaN and GaAs but it does not seem to present any benefit when applied to InP as we have run a few processes with this combined chemistry on InP without successful results.

To summarize, fluorinated gases alone are not suitable for etching III–V compound semiconductors due to the poor volatility of element III-fluorides (much higher T_B) compared to the corresponding element III-chloride. On the other hand, elements V-fluoride are more volatile than their corresponding chloride due to a much lower T_B .

In the case where the compound semiconductor contains Al atoms, the fluorine–chlorine combination is no longer suitable for etching the Al-containing material. Even at low fluorine flow, AlF_3 (with a formation enthalpy of $-1510 \text{ kJ mol}^{-1}$) is preferably formed instead of AlCl_3 (formation enthalpy of -704 kJ mol^{-1}) and as AlF_3 is not volatile (boiling point of 1291 °C versus 183 °C for AlCl_3) Al-containing material cannot be etched in a fluorinated chemistry. Hence, it is very common to use this combination as a selective dry etching to etch GaAs versus AlGaAs [18–21] and GaAs versus InGaP [20], where very high selectivity (>100 : 1) is reported. For the reasons explained above, a Cl–F combination should also etch GaN selectively versus AlGaN layers.

So far, an explanation was given for the enhanced etching rate with a combined fluorine and chlorine chemistry but an explanation is still required to explain why SiF_4 has not enhanced the etching rate of GaN [12]. For this, let us consider the dissociation energy of the gases used, which is defined as the energy required to dissociate one Cl- or F-atom from the chlorinated or the fluorinated gas, respectively, as shown in table 2.

Table 2. Dissociation enthalpy of the four gases used where the very high value of SiF₄ is inefficient in enhancing the etching rate of GaN [10].

	SiCl ₄	BCl ₃	SF ₆	SiF ₄
Dissociation enthalpy (kcal mol ⁻¹)	94.1	110.7	93.6	145.4

Table 2 shows that SiCl₄ is easier to ionize than BCl₃, or in other terms, at a well-defined power level, the density of reactants would be higher in a SiCl₄ discharge than in BCl₃. This would explain why the combination of BCl₃ and SF₆ [13] results in a lower etching rate than the combination of SiCl₄ and SF₆ [14]. Similar results were achieved by Pearton *et al.*, where higher etching rate of GaAs with Cl₂ : Ar compared to SiCl₄ : Ar were reported [22]. Note that the dissociation energy of Cl₂ is about 58 kcal mol⁻¹, whereas that of SiCl₄ is 94.1 kcal mol⁻¹; hence it is much easier to ionize Cl₂ than SiCl₄, which explains the difference in etching rate. Furthermore, adding SiF₄ to the chlorinated gas [12] does not result in any increase of the GaN etching rate. This suggests that SiF₄ with its very high dissociation energy (145 kcal mol⁻¹) was not dissociated and hence not contributing to the etching process. In other words, it seems that SiF₄ is not ionized in the discharge and as such does not improve the etching rate with the combined Cl- and F-chemistry. The dissociation energy gives a plausible explanation of the GaN etching rates found in the three papers discussed.

To summarize, adding SF₆ to SiCl₄ : Ar resulted in a four-fold increase of the etching rate of GaN; moreover, when we investigated the boundary chemistry conditions, as shown in table 3, a logical conclusion would be that this chemistry has a high chemical etching component.

The high etching rate for the Cl₂ : SF₆ gas chemistry is a clear indication of the high chemical nature of the etching process. This has been further demonstrated when etching bulk GaN (Ga- and N-polar) samples for 6 min using SiCl₄ : Ar : SF₆ (10 : 10 : 2 sccm) at 105 W and 40 mTorr. Polarity is not present in Si single crystals, whereas III-V semiconductors show polarity differences along directions where the planes contain only element III or element V atoms. III-V are similar to Si in being characterised by sp³-type bonds (each atom is connected to four first neighbours upon a tetrahedral shape; however, in GaAs one Ga is bonded to four As atoms and vice versa. This particularity results in a polarity phenomenon along the (1 1 1) planes in zinc blend (cubic) crystals and the c-direction in hexagonal lattices like GaN. Planes (1 1 1) are either A-type if ending with element III (like Ga) or B-type when ending with element V (like As). In plane (1 1 1)A each Ga atom is bonded to three As atoms in the underlying layer, hence this is Ga-polar and likewise (1 1 1)B is As-polar. In hexagonal structures this polarity is encountered along the c-plane where we can distinguish between Ga-polar in one direction and N-polar in the opposite direction in the same material.

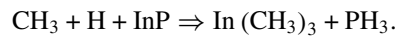
The average roughness of Ga-polar GaN was improved going from 2 nm down to 0.4 nm [23] and this etching has allowed the epitaxy of very high quality GaN/AlGaN layers on such smooth and clean bulk Ga-polar GaN [24]. Another

indication of the chemical character of this dry etching process is the higher etching rate of N-polar GaN (165 nm min⁻¹) as compared to that of Ga-polar GaN (110 nm min⁻¹ [23]). It is well known that N-polar GaN is chemically active due to the presence of two electrons on the outer shell of nitrogen atoms available for chemical reactions and hence it can be wet etched, for instance, in concentrated KOH solution at high temperature. Conversely, it is not possible to wet etch Ga-polar GaN due to the absence of any available electrons on its outer shell.

4.2. RIE of other III-V semiconductors

RIE of III-V semiconductors has been extensively reported in the literature and we can distinguish two main chemistries: the halogen-free chemistry of CH₄ : H₂ and Cl₂-based chemistries.

4.2.1. CH₄ : H₂ chemistry. This gas mixture is often used in etching InP-based materials and offers the advantage of low-risk chemistry (non-toxic but flammable), relatively low plasma damage and a good control of etching depth due to a low, but controllable, etching rate. In a CH₄ : H₂ plasma discharge the species that contribute to the etching process are the free radicals CH₃ and H, whereas the reaction products are trimethyl indium and phosphine, which are both volatile at low temperatures. The main reaction is

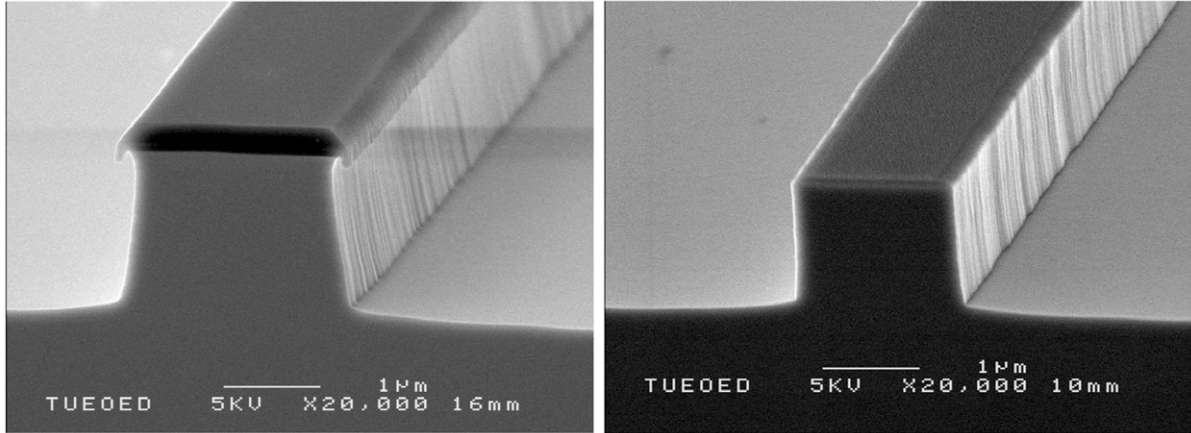
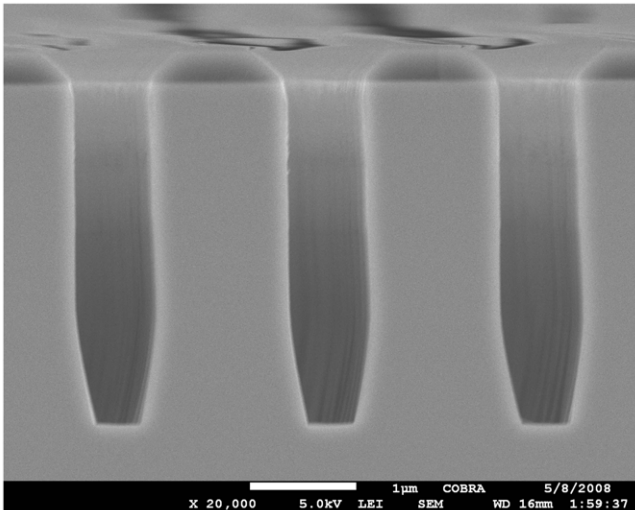


This chemistry has a major drawback as excessive polymer deposition takes place, which can disturb the etching process and worsen the etching morphology. Therefore this chemistry is often alternated with O₂ plasma to control the build-up of polymers in such a way that the resulting etch delivers smooth sidewalls while the number of cycles determines the etching depth. Figure 11 shows SEM micrographs of two etched InP samples in CH₄ : H₂, one without alternating O₂ plasma and the second with alternating O₂ plasma.

The etching rate of this gas combination is strongly dependent on the III-V materials. For instance, InP is typically etched at 20–30 nm min⁻¹ whereas the rate can easily decrease when replacing In atoms by Ga or Al atoms and also when replacing P atoms by As or Sb atoms. This chemistry has been extensively used in etching InP/InGaAsP materials [25] to fabricate micro-disks [26], nanostructures [27] and also InP-based integrated optics [28, 29]. This is mainly due to the smooth etched sidewalls ensuring low-loss waveguides in addition to the good control of etching depth. This chemistry can also be used in an ICP configuration where etch depth control can be associated with very smooth morphology, as shown in figure 12. Process details are 50 cycles of CH₄/H₂: 30/10 sccm, ICP/RF 200/110 W, 18 mTorr, 1 min, 200 °C alternated with 10 s O₂ (40 sccm) plasma at similar conditions. However, as can be seen in figure 12, this chemistry, even in an ICP configuration, is not suitable for etching high aspect ratios with much smaller dimensions, such as in PhCs—the unsuitability of this chemistry for PhC patterns has been confirmed by other authors [30]. One final remark on this chemistry is that when used in a high-density plasma system (ICP or ECR), the remote plasma source should be kept at a low power level. If the ICP/ECR power is too high it

Table 3. Etching rate of GaN at the boundary conditions of gas flows of the three used gases.

Gases	Ar	Ar : SF ₆	SiCl ₄ : Ar	SiCl ₄ : SF ₆	SiCl ₄ : Ar : SF ₆
Flow (sccm)	10	10 : 2	10 : 10	10 : 2	10 : 10 : 2
Etching rate (nm min ⁻¹)	9	11	22	80	95

**Figure 11.** InP etched non-stop for 30 min in CH₄ : H₂ (left) and with alternating short O₂ plasma (right).**Figure 12.** InP etching in a CH₄ : H₂ ICP process using 400 nm of SiO_x as a masking layer.

would inevitably lead to faster desorption of phosphor atoms, leaving behind indium clusters that will degrade the surface morphology after etching [31].

4.2.2. Cl₂-based chemistry. Cl₂-based chemistry, with its sub-variants, is used to etch GaAs-, InP- and GaN-based structures for various device applications. The main etching component is the chlorine radical which reacts with all III and V elements. Many sub-variants can be considered depending on the application. H₂ is commonly added as a passivation agent that allows better anisotropy and smoother side walls. This is very important for etching waveguides (integrated optics and lasers). Alternatively, methane can also be added to the Cl₂ : H₂ combination for additional passivation but this will

slow down the etching rate and at the same time deteriorate the selectivity towards the used mask. Another alternative to the Cl₂ : H₂ mixture is adding a small amount of Ar, which can better balance the physical etching and the passivation, resulting in high anisotropy and smooth sidewalls. When Al is one of the III-elements the Cl₂ : CH₄ : H₂ is one possibility but more commonly BCl₃ or SiCl₄ can be added to Cl₂. Another common combination is Cl₂ : O₂, which is a popular chemistry for achieving a high aspect ratio as in PhC-type patterns, where holes are typically in the range of 200–300 nm diameter with a required etching depth of 3 μm or more. Adding oxygen to chlorine enhances the ionisation percentage of Cl₂ in addition to the passivation role that it plays, resulting in a very high aspect ratio and smooth sidewalls. In this etching, a major part of the hole is cylindrical while the bottom part has more of a conical shape, often described as a carrot-like shape.

4.2.3. Cl₂ : CH₄ : H₂. This chemistry results in a smooth and moderate etching rate making it very suitable for etching passive waveguides for integrated optics (shown in figure 13). The starting process details are as follows:

- Cl₂ : CH₄ : H₂ (7 : 8 : 5.5 sccm),
- ICP/RF powers of 1000/100 W,
- 4 mT and at T = 200 °C (lower electrode).

The etching rates of InP and SiN_x were 1.2 μm min⁻¹ and 0.12 μm min⁻¹, respectively; hence a selectivity of 10 : 1 was achieved without any particular optimization. Some fine tuning of this process was carried out to fabricate low-loss deeply etched InGaAsP ($\lambda = 1.25 \mu\text{m}$) waveguides, and the lowest transmission losses (1 dB cm⁻¹ for TE light) were achieved at ICP/RF powers of 800/50 W [32]. An alternative chemistry could be Cl₂ : CH₄ : Ar, where the ratio of methane to chlorine seems crucial in obtaining vertical and smooth sidewalls [33].

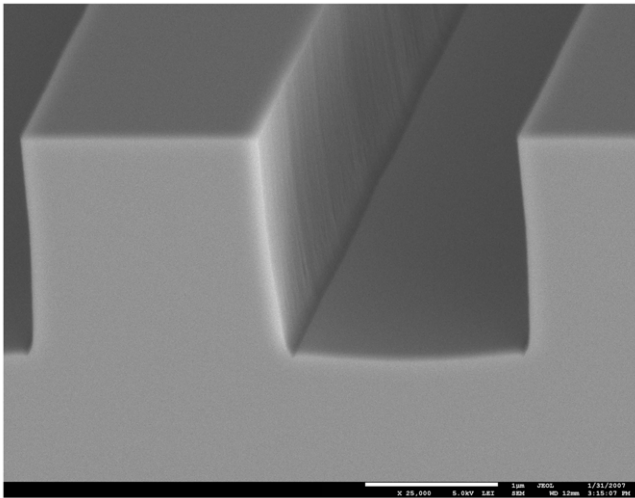


Figure 13. Smooth etched InP surface and sidewalls using Cl_2 , CH_4 , H_2 (7.8, 5.5 sccm), at ICP/RF powers of 1000/100 W, 4 mTorr and at a lower electrode T of 60°C for 1 min.

However, this chemistry was not satisfactory at all when we attempted to use it for fabricating high aspect ratio structures like PhC holes or DBR gratings.

4.2.4. $\text{Cl}_2 : \text{Ar} : \text{H}_2$. This chemistry, exempt of methane, has the advantage of being polymer-free and as such it is very suitable for etching InP-based materials. The role of hydrogen is to introduce a passivation effect, which helps achieve the desired etching shape. Figure 14 shows the influence of the H_2 flow when added to $\text{Cl}_2 : \text{Ar}$ at RF/ICP powers of 120/1000 W at 4 mTorr and electrode T of 160°C . With 3 sccm of H_2 the etching was rather isotropic and the tips ended in a conical shape, whereas with 12 sccm H_2 sufficient sidewall passivation takes place, ensuring a highly anisotropic etching with almost vertical and smooth sidewalls.

The effect of increased hydrogen flow in slowing down the etching rate has been well reported in the literature [34, 35]. The optimized gas flow was found to be $\text{Cl}_2 : \text{Ar} : \text{H}_2$ (7 : 4 : 12 sccm). The etching rate of InP of $1.4 \mu\text{m min}^{-1}$ was recorded, while SiO_x was etched at 100 nm min^{-1} leading to a very respectable etching selectivity of 14 : 1 and smooth sidewalls, with the exception of the 100 nm top area where an erosion (faceting) effect is visible. Bae *et al* [35] reported a way to eliminate this erosion by depositing a 50 nm thick PECVD SiO_x layer on top of the patterned NiCr/SiO_x which is etched away in the first 20–30 s of the etching process. Moreover, they demonstrate a clever patterning to enable AFM measurements of sidewall roughness using staggered ridges [35]. Parker *et al* [36] also reported smooth and vertical sidewalls in InP/InGaAsP structures. Note that the optimum H_2 to Cl_2 ratio is not universal but machine-dependent; hence it is necessary to perform such a flow sweep of hydrogen to determine optimum etching conditions in a particular machine.

To achieve high aspect ratio structures like PhC pillars and DBR grating mirrors, a standard technology using a ZEP520A resist on top of 400 nm SiN_x failed, as a thicker and more resistant mask was required to achieve the sub- μm patterns. A

simple trick to enable the etching of a thicker masking layer is to use three-level masking; i.e. add an intermediate metal layer that is resistant to fluorine plasma. The intermediate metal layer can be chromium or aluminum, with both metal fluorides being non-volatile. Hence, this three-level technology was then developed using a 50 or 60 nm Cr layer on top of 500 nm SiO_x [37]. In the case of PhC pillars the 50 nm high Cr circles were obtained using a PMMA layer (950k A4) lift-off process. The Cr is a good and sufficient masking material for etching the 500 nm SiO_x followed by removing the residual Cr layer in high-pressure O_2 plasma (barrel etcher or ashing system) to avoid any possible micro-masking by metal sputtering. Subsequently the InP was etched for 3 min, resulting in an etching depth of about $4 \mu\text{m}$. This process is very suitable for InP-based integrated optics, as demonstrated below:

- A very compact and low-loss polarization filter in InP-based PhC pillars was demonstrated [38].
- Very high quality DBR gratings in InP-based heterostructures were obtained that led to the fabrication of discrete tuneable lasers based on the filtered feedback effect [39].

4.2.5. Cl_2/O_2 for PhC (hole) technology. In developing the technology and process for PhC hole-type structures with high aspect ratio, the $\text{Cl}_2/\text{Ar}/\text{H}_2$ chemistry quickly shows its limitations. Alternative chemistries were required to achieve these $>10 : 1$ aspect ratio structures in semiconductor materials. Coldren and Rentschler [40] reported the use of Cl_2/O_2 chemistry for vertical wall dry etching of InP/InGaAsP at low pressures (1–2 mTorr), and other chemistries reported in literature include $\text{Cl}_2 : \text{N}_2$ [41]. We investigated the effect of oxygen, as it offered a good choice of an additive gas to Cl_2 to achieve the required aspect ratio. The addition of O_2 seems beneficial on two fronts: it enhances the ionisation state of the chlorine gas by providing more radicals to the etching process, and at the same time provides oxidation of the etched surface that enhances device quality through better passivation. Such a process is reported in [42, 43] for etching PhC holes in InP/InGaAsP heterostructures using $\text{Cl}_2 : \text{O}_2$ (14 : 2 sccm) at 1.2 mTorr, 1000/160 W ICP/RF at 200°C and etching for 1 min. The mask used was 400 nm of PECVD SiN_x . This mask will not allow any further etching as barely 100 nm of the mask remained. We applied the three-level masking technique described above to this technology. The starting mask was a 500 nm PECVD SiO_x layer and 50 nm of Cr. Next, the EBL patterning using ZEP resist Cr was first etched using the $\text{Cl}_2 : \text{O}_2$ ICP process, then the SiO_x was etched using the CHF_3 RIE process. Subsequently, and after removing the remaining Cr, the PhC patterns were etched using the same $\text{Cl}_2 : \text{O}_2$ process [42]. SEM inspection revealed a strong aspect ratio of 18 : 1 and the top of the PhC holes were free of any notching/faceting, as can be seen in figure 15.

5. Conclusions

We have described general but important aspects of RIE such as anisotropy, loading effect, lag effect, dc bias, choice of chemistry and performed an extensive experimental study on

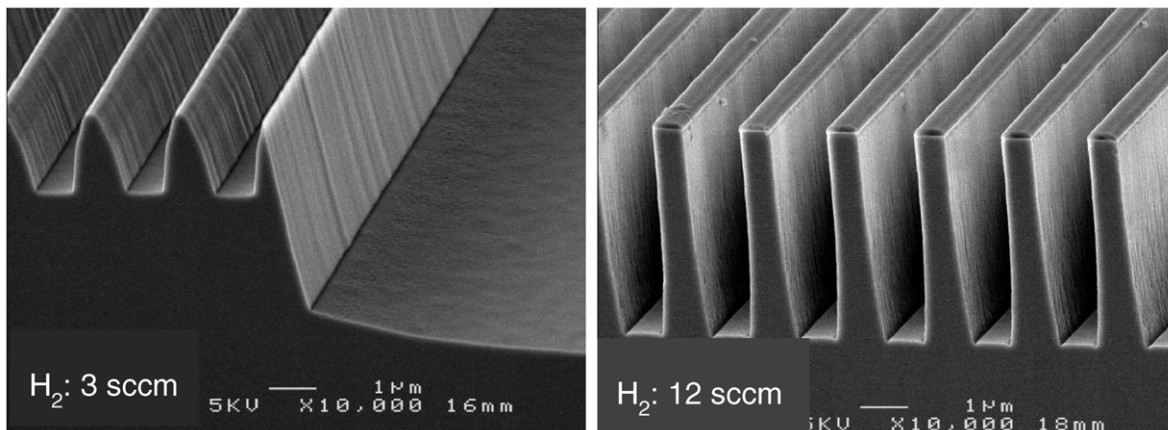


Figure 14. Influence of H₂ flow on sidewall passivation with only 3 sccm H₂ (left) leading to heavy lateral etching causing the full removal of the complete 400 nm SiN_x mask used in this etching, while 12 sccm H₂ is used in conjunction with the 600 nm SiN_x mask (right).

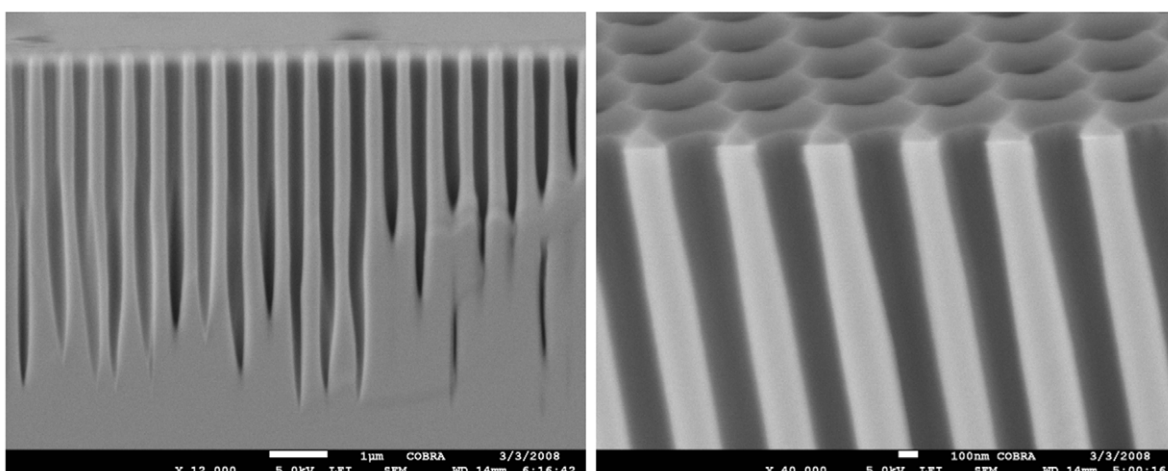


Figure 15. Very high aspect ratio PhC in InP material, demonstrating the potential of the three-level masking technology. The photograph on the right is a close-up of the same sample in a tilted position (25°).

micro-masking, where we demonstrated how to avoid typical micro-masking in etching InP-based materials. After a brief section on RIE of Si, SiO_x and SiN_x, a detailed study of etching GaN is presented, including a large discussion section explaining the four-fold increase in the etching rate of GaN when introducing SF₆ to a chlorinated gas, using a simple approach and backed up by thermodynamical data. Finally, four chemistries are reviewed and discussed for etching InP-based structures for use in photonic applications.

NB: Unless otherwise indicated, all experimental data shown in this paper have been obtained using a load-locked Oxford Plasma technology 100 system with an 180 mm ICP source at the Technical University Eindhoven in the Netherlands.

Acknowledgments

The author acknowledges fruitful discussion with Kaushal Vora and Jeff Kealley from the Australian National University in Canberra. He is also grateful to the Technical University Eindhoven for his past appointment and to the Australian

National Fabrication Facility through the NCRIS initiative for financial support.

References

- [1] Lieberman M A and Lichtenberg A J 2005 *Principles of Plasma Discharges and Materials Processing* 2nd edn (New York: Wiley) chapters 11, 12, 15, 16
- [2] Mogab C J 1977 The loading effect in plasma etching *J. Electrochem. Soc.* **124** 1262–8
- [3] Legtenberg R, Jansen H, De Boer M and Elwenspoek M 1995 Anisotropic reactive ion etching of silicon using SF₆/O₂/CHF₃ as mixtures *J. Electrochem. Soc.* **142** 2020–8
- [4] Im Y H and Hahn Y B 2002 Heat transfer between wafer and electrode in a high density plasma etcher *Korean J. Chem. Eng.* **19** 347–50
- [5] Lide D R (ed) 2006–2007 *CRC Handbook of Physics and Chemistry* 87th edn (Boca Raton, FL: CRC Press)
- [6] Carlström C F and Karouta F 2014 unpublished
- [7] Karouta F, Geluk E J, van der Heijden R W, Silov A Yu, Eijkemans T, van der Tol J J G M, Smit M K and Salemink H W M 2004 Influence of ICP etching on surface morphology of InP substrates *Proc. IPRM (Kagoshima, 31 May–4 June 2004)* pp 322–325

- [8] Kang S-Y, Lee S K, Lee H J, Kwon K H, Choi B G, Song Y H, Lee J H and Cho K I 1999 Fluorine incorporation effects in Cl₂ plasma etching of silicon: quadrupole mass spectrometer analysis *J. Electrochem. Soc.* **146** 4626–9
- [9] McAllister D V, Wang P M, Davis S P, Park J H, Canatella P J, Allen M G and Prausnitz M R 2003 Microfabricated needles for transdermal delivery of macromolecules and nanoparticles: fabrication methods and transport studies *Proc. Natl Acad. Sci. USA* **100** 13755–60
- [10] Kok K W, Yoo W J, Sooriakumar K, Sheng Pan J and Lee E Y 2002 Investigation of *in situ* trench etching process and Bosch process for fabricating high-aspect-ratio beams for microelectromechanical systems *J. Vac. Sci. Technol. B* **20** 1878
- [11] Chang C, Wang Y F, Kanamori Y, Shih J J, Kawai Y, Lee C K, Wu K C and Esashi M 2005 Etching submicrometer trenches by using the Bosch process and its application to the fabrication of antireflection structures *J. Micromech. Microeng.* **15** 580
- [12] Adesida I, Mahajan A, Andideh E, Asif-Khan M, Olsen D T and Kuznia J N 1993 Reactive ion etching of gallium nitride in silicon tetrachloride plasmas *Appl. Phys. Lett.* **63** 2777–9
- [13] Feng M S, Guo J D, Lu Y M and Chang E Y 1996 Reactive ion etching of GaN with BCl₃/SF₆ plasmas *Mater. Chem. Phys.* **45** 80–3
- [14] Karouta F, Jacobs B, Vreugdewater P, van Melick N G H, Schoen O, Protzmann H and Heuken M 1999 High etch rate and smooth morphology using a novel chemistry in reactive ion etching of GaN *Electrochem. Solid State Lett.* **2** 240–1
- [15] Karouta F, Jacobs B, Schoen O and Heuken M 1999 Chemical and complementary role of fluorine in a chlorine based reactive ion etching of GaN *Phys. Status Solidi a* **176** 755–8
- [16] http://en.wikipedia.org/wiki/Nitrogen_trifluoride
- [17] Nordheden K J, Upadhyaya K, Lee Y S, Gogineni S P and Kao M Y 2000 GaAs etch rate enhancement with SF₆ addition to BCl₃ plasmas *J. Electrochem. Soc.* **147** 3850–2
- [18] Hikosaka K, Mimura T and Joshi K 1981 Selective dry etching of AlGaAs–GaAs heterojunction *Japan J. Appl. Phys.* **20** L847–50
- [19] Salimian S and Cooper C B 1988 Selective dry etching of GaAs over AlGaAs in SF₆/SiCl₄ mixtures *J. Vac. Sci. Technol. B* **6** 1641–4
- [20] Hays D C *et al* 2000 High selectivity inductively coupled plasma etching of GaAs over InGaP *Appl. Surf. Sci.* **156** 76–84
- [21] Lee J W, Devre M W, Reelfs B H, Johnson D and Sasserath J N 2000 Advanced selective dry etching of GaAs/AlGaAs in high density inductively coupled plasmas *J. Vac. Sci. Technol. A* **18** 1220–4
- [22] Pearton S J, Chakrabarti U K, Hobson W S and Kinsella A P 1990 Reactive ion etching of GaAs, AlGaAs and GaSb in Cl₂ and SiCl₄ *J. Vac. Sci. Technol. A* **4** 607–17
- [23] Karouta F, Weyher J L, Jacobs B, Nowak G, Presz A, Grzegory I and Kaufmann L M F 1999 Final polishing of Ga-polar GaN substrates reactive ion etching *J. Electron. Mater.* **28** 1448–51
- [24] Weyher J L, Zauner A, Brown P D, Karouta F, Wysmolek A, Hageman P R and Prorowski S 1999 Growth of high quality Ga-polar GaN after novel reactive ion etching *Phys. Status Solidi a* **176** 573–7
- [25] Hayes T R, Dreisbach M A, Thomas P M, Dautremont-Smith W C and Heimbrock L A 1989 Reactive ion etching of InP using CH₄/H₂ mixtures: mechanisms of etching and anisotropy *J. Vac. Sci. Technol. B* **7** 1130–40
- [26] Choi S J, Djordjev K, Choi S J and Dapkus P D 2002 CH₄-based dry etching of high Q InP microdisks *J. Vac. Sci. Technol. B* **20** 301–5
- [27] Adesida I, Nummila K, Andideh E, Hughes J, Caneau C, Bhat R and Holmstrom R 1990 Nanostructure fabrication in InP and related compounds *J. Vac. Sci. Technol. B* **8** 1357–60
- [28] den Besten J H, Broeke R G, van Geemert M, Binsma J J M, Heinrichsdorff F, Dongen T, Bente E A J M, Leijtens X J M and Smit M K 2003 An integrated 4 × 4-channel multiwavelength laser on InP *IEEE Photon. Technol. Lett.* **15** 368–70
- [29] Hill M T *et al* 2007 Lasing in metallic-coated nanocavities *Nature Photon.* **1** 589–94
- [30] Mulot M, Anand S, Carlström C F, Swillo M and Talneau A 2002 Dry etching of photonic crystals in InP based materials *Phys. Scr.* **T101** 106–9
- [31] Pearton S J, Chakrabarti U K, Kinsella A P, Johnson D and Constantine C 1990 Electron cyclotron resonance plasma etching of InP in CH₄/H₂/Ar *Appl. Phys. Lett.* **56** 1424–6
- [32] Karouta F, Zhu Y C, Geluk E J, van der Tol J J G M, Binsma J J M and Smit M K 2003 ICP etching of InP and its applications in photonic circuits *Proc. SPIE* **5277** 22–8
- [33] Vodjdani N and Parrens P 1987 Reactive ion etching of GaAs with higher aspect ratios with Cl₂–CH₄–H₂–Ar mixtures *J. Vac. Sci. Technol. B* **5** 1591–8
- [34] Rommel S L *et al* 2002 Effect of H₂ on the etch profile of InP/InGaAsP alloys in Cl₂/Ar/H₂ inductively coupled plasma reactive ion etching chemistries for photonic device fabrication *J. Vac. Sci. Technol. B* **20** 1327–30
- [35] Bae J W, Zhao W, Jang J H, Adesida I, Lepore A, Kwakernaak M and Abeles J H 2003 Characterization of sidewall roughness of InP/InGaAsP etched using inductively coupled plasma for low loss optical waveguide applications *J. Vac. Sci. Technol. B* **21** 2888–91
- [36] Parker J S, Norberg E J, Guzzon R S, Nicholes S C and Coldren L A 2011 High verticality InP/InGaAsP etching in Cl₂/H₂/Ar inductively coupled plasma for photonic integrated circuits *J. Vac. Sci. Technol. B* **29** 011016
- [37] Karouta F, Docter B, Geluk E J, Sander-Jochem M J H, van der Tol J J G M and Smit M K 2005 Role of temperature and gas chemistry in micro-masking on InP by ICP etching *18th Annual LEOS Meeting (THDD2)* (Sydney, 23–27 October 2005) pp 987–8
- [38] Kok A, Geluk E J, Karouta F, van der Tol J J G M, Baets R and Smit M K 2008 Short polarization filter in pillar-based photonic crystals *IEEE Photon. Technol. Lett.* **20** 1369–71
- [39] Docter B, Pozo J, Beri S, Ermakov I V, Danckaert J, Smit M K and Karouta F 2010 Discretely tunable laser based on filtered feedback for telecommunication applications *IEEE J. Sel. Top. Quantum Electron.* **16** 1405–12
- [40] Coldren L A and Rentschler J A 1981 Directional reactive ion etching of InP with Cl₂ containing gases *J. Vac. Sci. Technol. B* **19** 225–30
- [41] Strasser P, Wuest R, Robin F, Erni D and Jackel H 2007 Detailed analysis of the influence of an inductively coupled plasma reactive-ion etching process on the hole depth and shape of photonic crystals in InP/InGaAsP *J. Vac. Sci. Technol. B* **25** 387–93
- [42] Carlström C F, van der Heijden R, Karouta F, van der Drift E, van der Heijden R W and Salemink H W M 2006 Cl₂/O₂-inductively coupled plasma etching of deep hole-type photonic crystals in InP *J. Vac. Sci. Technol. B* **24** L6
- [43] Carlström C F, van der Heijden R, Andriesse M S P, Karouta F, van der Heijden R W, van der Drift E and Salemink H W M 2008 Comparative study of Cl₂, Cl₂/O₂ and Cl₂/N₂ inductively coupled plasma processes for etching of high aspect ratio photonic crystal holes in InP *J. Vac. Sci. Technol. B* **26** 1675–83